

# Distributed optimal control of lambda-omega systems

Alfio Borzi\*      Roland Griesse†

## Abstract

The formulation, analysis, and numerical solution of distributed optimal control problems governed by lambda-omega systems is presented. These systems provide a universal model for reaction-diffusion phenomena with turbulent behavior. Existence and regularity properties of solutions to the free and controlled lambda-omega models are investigated. To validate the ability of distributed control to drive lambda-omega systems from a chaotic to an ordered state, a space-time multigrid method is developed based on a new smoothing scheme. Convergence properties of the multigrid scheme are discussed and results of numerical experiments are reported.

**Keywords:** Lambda-omega systems, optimal control, multigrid methods.

**AMS:** 35K57, 49J20, 49K20, 65M06, 65M55.

## 1 Introduction

Lambda-omega ( $\lambda - \omega$ ) systems represent a ‘universal model’ to investigate chemical reaction processes [19], to describe the time evolution of biological systems [27], to analyze the mechanism of pattern formation [6], and to study the onset of turbulent behavior [25]. An example of an emerging technological application based on pattern forming systems is given by memory

---

\*Institute of Mathematics, University of Graz, Heinrichstr. 36, A-8010 Graz, Austria  
([alfio.borzi@uni-graz.at](mailto:alfio.borzi@uni-graz.at))

†Johann Radon Institute for Computational and Applied Mathematics (RICAM), Austrian Academy of Sciences, Altenbergerstr. 69, A-4040 Linz, Austria  
([roland.griesse@oeaw.ac.at](mailto:roland.griesse@oeaw.ac.at))

devices using magnetic domain patterns [7]. In this and many other applications, it is often required to act on the given reaction diffusion system to drive it towards a desired state or to optimize some process modeled by the system.

Considering the importance of possible applications related to controlled lambda-omega models, we present in this paper the formulation, analysis, and numerical solution of optimal control problems governed by a representative  $\lambda - \omega$  system. We focus on distributed control since, apparently, only this control mechanism can effectively influence the system. Distributed control can be realized, e.g., by laser pulses, magnetic fields, injection/suction of species, etc.. In the context of chemical reactions involving ionic species, the control may stand for an electric field applied to drive the system to form a desired conductivity pattern [14].

Concerning the theoretical investigation of reaction-diffusion systems related to  $\lambda - \omega$  models see [21,31–33] and references given there. We contribute to this research by proving, in an appropriate functional setting, existence and regularity properties of solutions to the  $\lambda - \omega$  system subject to homogeneous Dirichlet or Neumann boundary conditions.

For the optimal control formulation of reaction diffusion systems, relatively few results are available; see, e.g., [23, 24, 28]. In particular, we mention [17,18] for optimal control problems of single-species equations, and [15] for an optimal control problem of a phase-field equation. In [12], optimal control of a two-species reaction-diffusion model with monotone nonlinearities has been considered. In contrast lambda-omega systems possess non-monotone nonlinearities. For this class of problems, we prove existence of solutions to the corresponding optimal control problems with distributed control. Although the system may be chaotic, the control-to-state map is continuous and even differentiable.

It is the second goal of this paper to numerically validate the ability of distributed control to drive the  $\lambda - \omega$  system from a chaotic to an ordered state. To this end, we propose an efficient space-time multigrid solver for reaction-diffusion optimal control problems capable of handling the chaotic dynamics. In this setting, we expect that otherwise efficient approaches such as proper orthogonal decomposition or adaptive grid refinement techniques may not achieve their maximum performance.

In the following section, lambda-omega systems are introduced and analyzed. Existence, uniqueness, and smoothness properties of solutions are proved. In Section 4, we introduce a class of optimal control problems for

the  $\lambda - \omega$  system and derive its first-order necessary and second-order sufficient optimality conditions. Existence of global optimal solutions is proved. In Section 5 we describe the discretization of the optimality system and its solution by a new space-time multigrid scheme suitable for time-dependent multi-species reaction-diffusion optimality systems. In particular we focus on the formulation and properties of a new smoother. In Section 6, by means of the multigrid algorithm, we elaborate on numerical experiments to validate the present optimal control formulation. Some concluding remarks complete the exposition of this paper.

## 2 Lambda-omega systems

General two-species reaction-diffusion systems are of the form

$$\partial y_1 / \partial t = F_1(y_1, y_2; \beta) + \sigma \Delta y_1, \quad (1)$$

$$\partial y_2 / \partial t = F_2(y_1, y_2; \beta) + \sigma \Delta y_2, \quad (2)$$

where  $F_1$  and  $F_2$  are nonlinear functions modelling reaction kinetics,  $\beta$  is a reaction parameter, and  $\sigma > 0$  is the diffusion coefficient. Of particular importance for modelling life-systems are reaction-diffusion equations where the reaction kinetics exhibit a periodic limit cycle behavior via a Hopf bifurcation. In this case, in the vicinity of the Hopf bifurcation, systems of the type (1)–(2) are similar to lambda-omega systems; see [10]. Lambda-omega systems are of the form

$$\frac{\partial}{\partial t} \begin{pmatrix} y_1 \\ y_2 \end{pmatrix} = \begin{bmatrix} \lambda(s) & -\omega(s) \\ \omega(s) & \lambda(s) \end{bmatrix} \begin{pmatrix} y_1 \\ y_2 \end{pmatrix} + \sigma \Delta \begin{pmatrix} y_1 \\ y_2 \end{pmatrix}, \quad s^2 = y_1^2 + y_2^2, \quad (3)$$

where  $\lambda(s)$  and  $\omega(s)$  are real functions of  $s$ .

We focus on a representative functional form of  $\lambda$  and  $\omega$  which was proposed in [20] to model chemical turbulence; see also [27,31] and the references given there:

$$\lambda(s) = 1 - s^2 \text{ and } \omega(s) = -\beta s^2. \quad (4)$$

It is easy to show that  $|\beta|$  is the essential parameter so we assume  $\beta > 0$  in what follows. Equations (3)–(4) can also be written in their complex form

$$w_t = w - (1 + i\beta)|w|^2 w + \sigma \Delta w, \quad (5)$$

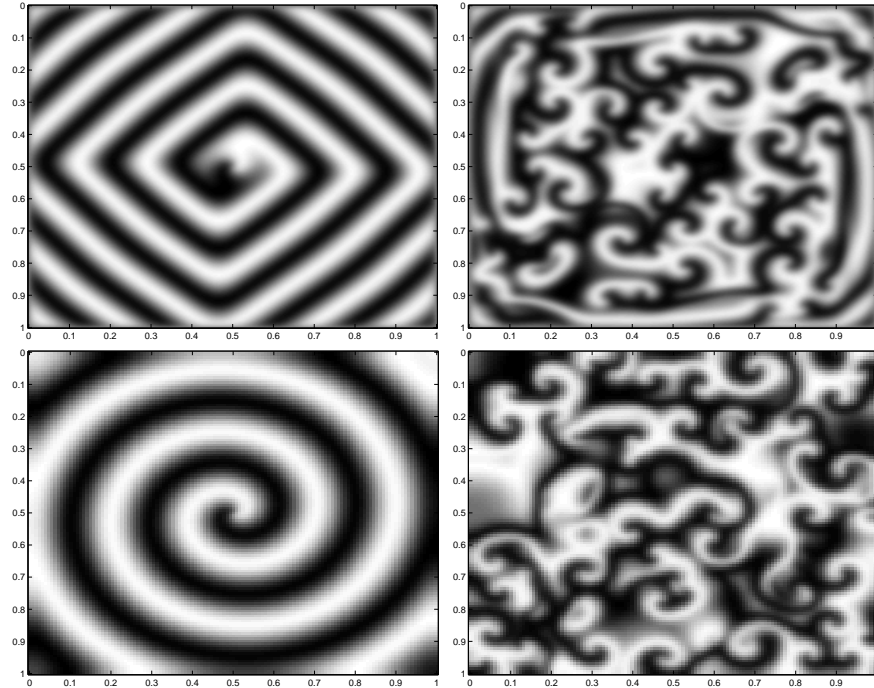


Figure 1: Solution  $y_1$  of (3)–(4) for  $\beta = 1$  (left) and  $\beta = 2$  (right) and  $\sigma = 10^{-4}$  with zero Dirichlet (top) and zero Neumann (bottom) boundary conditions, at  $t = 200$  and for  $(x_1, x_2) \in \Omega = (0, 1)^2$ . Dark regions correspond to negative values, bright regions correspond to positive values.

where  $w = y_1 + iy_2$ , which is a special case of the complex Ginzburg-Landau model; see, e.g., [33]. These equations have a long history in physics as a generic amplitude equation near the onset of instabilities that lead to chaotic dynamics in fluid mechanical systems.

System (3)–(4) possesses spiral wave solutions which persist indefinitely. In Figure 1, snapshots of uncontrolled solutions for the regular (left) and turbulent (right) regimes are presented. As  $\beta$  becomes larger than a threshold value, spiral wave solutions become unstable and nucleate spontaneously giving rise to turbulence. It is important to recognize that the occurrence of persistent spatio-temporal structures is possible because of instability inherent in the system. Roughly speaking, for a given domain  $\Omega$ , the diffusion rate  $\sigma$  has to be chosen sufficiently small in order to obtain persisting patterns. This is the focus in our numerical examples in Section 6 where we choose  $\sigma = 10^{-4}$  for  $\Omega = (0, 1) \times (0, 1)$ . On the other hand, the onset of

turbulence is due to instability of (pattern) solutions as  $\beta$  becomes large. For a detailed discussion and additional references, see, e.g., [3, 29].

### 3 Existence and uniqueness of solutions

Before addressing optimal control problems governed by (3)–(4), we first investigate the existence and uniqueness of solutions of the forward problem. Assume  $\Omega$  to be a sufficiently regular bounded domain in  $\mathbb{R}^2$ . For given final time  $T > 0$ , we denote by  $Q = \Omega \times (0, T)$  the space-time cylinder and by  $\Sigma = \partial\Omega \times (0, T)$  its lateral boundary. For convenience, let us rewrite below the  $\lambda - \omega$  system with source terms, which later represent the distributed control. We have

$$\frac{\partial}{\partial t} \begin{pmatrix} y_1 \\ y_2 \end{pmatrix} = \begin{bmatrix} 1 - (y_1^2 + y_2^2) & \beta(y_1^2 + y_2^2) \\ -\beta(y_1^2 + y_2^2) & 1 - (y_1^2 + y_2^2) \end{bmatrix} \begin{pmatrix} y_1 \\ y_2 \end{pmatrix} + \sigma \Delta \begin{pmatrix} y_1 \\ y_2 \end{pmatrix} + \begin{pmatrix} u_1 \\ u_2 \end{pmatrix}, \quad (6)$$

subject to homogeneous Neumann boundary conditions

$$\sigma \frac{\partial}{\partial n} \begin{pmatrix} y_1 \\ y_2 \end{pmatrix} = \begin{pmatrix} 0 \\ 0 \end{pmatrix} \quad \text{on } \Sigma, \quad (7a)$$

or homogeneous Dirichlet boundary conditions

$$\begin{pmatrix} y_1 \\ y_2 \end{pmatrix} = \begin{pmatrix} 0 \\ 0 \end{pmatrix} \quad \text{on } \Sigma, \quad (7b)$$

and initial conditions

$$\begin{pmatrix} y_1(\cdot, 0) \\ y_2(\cdot, 0) \end{pmatrix} = \begin{pmatrix} y_{10} \\ y_{20} \end{pmatrix} \quad \text{on } \Omega. \quad (8)$$

Let us prove that (6)–(8) has a unique solution in appropriately chosen spaces. As usual,  $L^p$ ,  $H^1$  and  $H_0^1$  are standard Sobolev spaces [1], and  $H^1(\Omega)^*$  and  $H^{-1}(\Omega)$  are the duals of  $H^1(\Omega)$  and  $H_0^1(\Omega)$ , respectively.

Since  $\Omega \subset \mathbb{R}^2$  and because of the presence of cubic nonlinearities, we consider—in contrast to the standard  $W(0, T)$ , see, e.g., [8, Chapter XVIII]—the higher order state space  $H^{2,1}(Q)$  given by

$$H^{2,1}(Q) = \{y \in L^2(0, T; H^2(\Omega)) : \partial y / \partial t \in L^2(0, T; L^2(\Omega))\},$$

in case of Neumann boundary conditions and

$$H^{2,1}(Q) = \{y \in L^2(0, T; H^2(\Omega) \cap H_0^1(\Omega)) : \partial y / \partial t \in L^2(0, T; L^2(\Omega))\}$$

in case of Dirichlet boundary conditions, endowed with the usual norm

$$\|y\|_{H^{2,1}(Q)} = \|y\|_{L^2(0, T; H^2(\Omega))} + \|y_t\|_{L^2(0, T; L^2(\Omega))}.$$

In the sequel, we shall use the shorter notation  $L^2(0, T; H^1)$  instead of  $L^2(0, T; H^1(\Omega))$ , etc.

Our proof of the Existence and Uniqueness Theorem below is based on the Leray-Schauder fixed-point theorem [11, p. 222], which we cite for convenience:

**Leray-Schauder Fixed-Point Theorem** *Let  $T$  be a compact operator of the Banach space  $B$  into itself. Suppose that for all  $s \in [0, 1]$ , there exists a constant  $M > 0$ , independent of  $s$ , such that  $y = s \cdot Ty$  implies that  $\|y\|_B \leq M$ . Then  $T$  has a fixed-point.*

Let us define the operator  $T$  by means of the relation  $v = Ty$  where  $v$  is the unique solution of the linear PDE system

$$\frac{\partial}{\partial t} \begin{pmatrix} v_1 \\ v_2 \end{pmatrix} = \begin{bmatrix} 1 - (y_1^2 + y_2^2) & \beta(y_1^2 + y_2^2) \\ -\beta(y_1^2 + y_2^2) & 1 - (y_1^2 + y_2^2) \end{bmatrix} \begin{pmatrix} v_1 \\ v_2 \end{pmatrix} + \sigma \Delta \begin{pmatrix} v_1 \\ v_2 \end{pmatrix} + \begin{pmatrix} u_1 \\ u_2 \end{pmatrix}, \quad (9)$$

subject to homogeneous Neumann boundary conditions and initial conditions  $v_i(\cdot, 0) = y_{i0} \in H^1(\Omega)$ , or Dirichlet boundary conditions and  $v_i(\cdot, 0) = y_{i0} \in H_0^1(\Omega)$ . For  $s \in \mathbb{R}$ ,  $v = s \cdot Ty$  holds if in (9),  $u_i$  is replaced by  $s \cdot u_i$  and  $y_{i0}$  is replaced by  $s \cdot y_{i0}$ .

**Proposition 1 (Properties of  $T$ )** *The operator  $T$  maps  $B = [H^{2,1}(Q)]^2$  into itself. Moreover,  $T$  is compact and satisfies the condition of the Leray-Schauder Theorem.*

The proof has been postponed to Appendix A.1 to improve readability. Our main result in this section is the following

**Theorem 2 (Existence and uniqueness)** *Given initial conditions  $y_{10}$ ,  $y_{20}$  in  $H^1(\Omega)$  in the case of Neumann boundary conditions and  $y_{10}$ ,  $y_{20}$  in  $H_0^1(\Omega)$  in the case of Dirichlet boundary conditions, and source terms  $u_1$ ,*

$u_2$  in  $L^2(Q)$ , there exists a unique solution  $(y_1, y_2)$  in  $[H^{2,1}(Q)]^2$  of (6)–(8) which satisfies the a priori estimate

$$\|y_1\|_{H^{2,1}(Q)} + \|y_2\|_{H^{2,1}(Q)} \leq p(\|y_{10}\|_{H^1(\Omega)}, \|y_{20}\|_{H^1(\Omega)}, \|u_1\|_{L^2(Q)}, \|u_2\|_{L^2(Q)}) \quad (10)$$

with some polynomial  $p : \mathbb{R}^4 \rightarrow \mathbb{R}$  of order 6.

We do not aim at obtaining a sharp a priori estimate as (10) suffices to show the boundedness of the states presuming the boundedness of the controls, see the proof of Theorem 4 below. The proof of Theorem 2 has been postponed to the Appendix A.2.

**Proposition 3 (The control-to-state map)** *The map  $[L^2(Q)]^2 \ni u \mapsto y(u) \in [H^{2,1}(Q)]^2$  defined by the unique solution of (6)–(8) is continuous and Fréchet differentiable.*

**Proof.** This property follows immediately from the implicit function theorem in Banach spaces [9, Theorem 15.1]: Note that the linearized problem

$$\begin{aligned} \frac{\partial}{\partial t} \begin{pmatrix} \bar{y}_1 \\ \bar{y}_2 \end{pmatrix} &= \begin{bmatrix} 1 - 3y_1^2 - y_2^2 + 2\beta y_1 y_2 & \beta y_1^2 + 3\beta y_2^2 - 2y_1 y_2 \\ -3\beta y_1^2 - \beta y_2^2 - 2y_1 y_2 & 1 - y_1^2 - 3y_2^2 - 2\beta y_1 y_2 \end{bmatrix} \begin{pmatrix} \bar{y}_1 \\ \bar{y}_2 \end{pmatrix} \\ &+ \sigma \Delta \begin{pmatrix} \bar{y}_1 \\ \bar{y}_2 \end{pmatrix} + \begin{pmatrix} f_1 \\ f_2 \end{pmatrix} \quad \text{in } Q \end{aligned} \quad (11)$$

with homogeneous Neumann or Dirichlet boundary conditions and initial conditions  $(\bar{y}_1(\cdot, 0), \bar{y}_2(\cdot, 0)) = (g_1, g_2)$  is easily seen to have a unique solution in  $[H^{2,1}(Q)]^2$  for all  $f_i \in L^2(Q)$  and all  $g_i \in H^1(\Omega)$  or  $g_i \in H_0^1(\Omega)$ , respectively, which depends continuously on the right hand side and initial data  $f_i$  and  $g_i$ .  $\square$

## 4 The optimal control problem

With the results from the previous section available, we are ready to discuss distributed optimal control problems governed by the  $\lambda - \omega$  system (6), where  $u_1$  and  $u_2$  are the control functions for the two species  $y_1$  and  $y_2$ . The purpose of the control is to let the system follow desired trajectories, represented by functions  $y_{id} \in L^2(Q)$ , and/or to reach desired terminal states,

denoted by functions  $y_{iT} \in L^2(\Omega)$ . ( $y_{id}$  and  $y_{iT}$  need not be attainable.) For this purpose, we take

$$J(y, u) = \sum_{i=1}^2 \left( \frac{\alpha_i}{2} \|y_i(\cdot, T) - y_{iT}\|_{L^2(\Omega)}^2 + \frac{\beta_i}{2} \|y_i - y_{id}\|_{L^2(Q)}^2 + \frac{\gamma_i}{2} \|u_i\|_{L^2(Q)}^2 \right), \quad (12)$$

as the objective function, where  $y = (y_1, y_2)$  and  $u = (u_1, u_2)$ , and the weights  $\alpha_i, \beta_i$  are nonnegative and  $\gamma_i$  is positive. To summarize, the optimal control problem under consideration is

$$\begin{aligned} \mathbf{OCP} \quad & \text{Minimize (12) over } (y, u) \in [H^{2,1}(Q)]^2 \times [L^2(Q)]^2 \\ & \text{such that the } \lambda - \omega \text{ system (6)–(8) is satisfied.} \end{aligned}$$

**Proposition 4 (Existence of a global optimal solution)** *There exists at least one global minimizer for OCP.*

**Proof.** We only sketch the main steps of the argument since we follow a common line of proof, cf. [28]. Let  $(y^n, u^n)$  be a minimizing sequence, i.e.,  $J(y^n, u^n)$  converges to the infimum of  $J(y, u)$  over all feasible  $(y, u)$ . Then  $\{u_i^n\}$  is bounded in  $L^2(Q)$ . By the a priori bound (10),  $\{y_i^n\}$  is also bounded in  $H^{2,1}(Q)$ . Thus we can extract weakly convergent subsequences. These satisfy the  $\lambda - \omega$  system (6)–(8) as can be shown by the same technique used in Proposition 1. Weak lower semi-continuity of  $J$  completes the proof.  $\square$

First-order necessary conditions are the basis for finding local optimal solutions. We now verify that if  $(y, u)$  is a local optimal solution for **OCP**, then there exists an adjoint state  $p$  such that the following first-order necessary conditions are satisfied.

**Proposition 5 (First-order necessary conditions)** *Let  $(y, u)$  be a local optimal solution for OCP. Let  $p$  be the unique solution in  $W(0, T)$  of the adjoint equation*

$$\begin{aligned} -\frac{\partial}{\partial t} \begin{pmatrix} p_1 \\ p_2 \end{pmatrix} &= \begin{bmatrix} 1 - 3y_1^2 - y_2^2 + 2\beta y_1 y_2 & -3\beta y_1^2 - \beta y_2^2 - 2y_1 y_2 \\ \beta y_1^2 + 3\beta y_2^2 - 2y_1 y_2 & 1 - y_1^2 - 3y_2^2 - 2\beta y_1 y_2 \end{bmatrix} \begin{pmatrix} p_1 \\ p_2 \end{pmatrix} \\ &+ \sigma \Delta \begin{pmatrix} p_1 \\ p_2 \end{pmatrix} - \begin{pmatrix} \beta_1(y_1 - y_{1d}) \\ \beta_2(y_2 - y_{2d}) \end{pmatrix} \quad \text{in } Q \quad (13) \\ \begin{pmatrix} p_1(\cdot, T) \\ p_2(\cdot, T) \end{pmatrix} &= - \begin{pmatrix} \alpha_1(y_1(\cdot, T) - y_{1T}) \\ \alpha_2(y_2(\cdot, T) - y_{2T}) \end{pmatrix} \quad \text{in } \Omega \end{aligned}$$

with Neumann or Dirichlet boundary conditions (the same as for the state equation). Then  $u$  and  $p$  satisfy

$$\gamma_1 u_1 - p_1 = 0 \quad \text{and} \quad \gamma_2 u_2 - p_2 = 0 \quad \text{on } Q.$$

**Proof.** The proof proceeds by defining the reduced objective  $\tilde{f}(u) = f(S(u), u)$  using the control-to-state map  $S$ , where  $u = (u_1, u_2)$ . We only sketch the main steps and refer, e.g., to [30] for details of this technique. A necessary condition for  $u$  to be a local minimizer is that the gradient of  $\tilde{f}$  vanishes.

Multiplying the adjoint equation (13) by the solution of the *linearized* state equation, integrating over  $Q$  and using integration by parts, we find that the Fréchet gradient of  $\tilde{f}$  is exactly  $(\gamma_1 u_1 - p_1, \gamma_2 u_2 - p_2)^\top$  from where the claim follows.  $\square$

In order to ensure the local optimality of a given state/control pair, one can invoke the following second-order sufficient conditions:

**Proposition 6 (Second-order sufficient conditions)** *Suppose that the state/control pair  $(y, u)$  and its adjoint state  $p$  satisfy the first-order necessary conditions (Proposition 5). For any given  $(\bar{u}_1, \bar{u}_2) \in [L^2(Q)]^2$ , let  $(\bar{y}_1(\bar{u}), \bar{y}_2(\bar{u}))$  be the unique solution of the linearized equation (11) with right hand side  $f_1 = \bar{u}_1$  and  $f_2 = \bar{u}_2$  and initial conditions  $g_1 = g_2 = 0$ . If all such pairs  $(\bar{y}, \bar{u})$  satisfy the estimate*

$$\begin{aligned} & \sum_{i=1}^2 \left( \frac{\alpha_i}{2} \|\bar{y}_i(\cdot, T)\|_{L^2(\Omega)}^2 + \frac{\beta_i}{2} \|\bar{y}_i\|_{L^2(Q)}^2 + \frac{\gamma_i}{2} \|\bar{u}_i\|_{L^2(Q)}^2 \right) \\ & + \int_Q (\bar{y}_1, \bar{y}_2)^\top \begin{pmatrix} 6y_1 & (2-\beta)y_2 - 2\beta y_1 \\ (2-\beta)y_2 - 2\beta y_1 & 2y_1 - 6\beta y_2 \end{pmatrix} \begin{pmatrix} \bar{y}_1 \\ \bar{y}_2 \end{pmatrix} p_1 \\ & + \int_Q (\bar{y}_1, \bar{y}_2)^\top \begin{pmatrix} 2y_2 + 6\beta y_1 & 2y_1 + 2\beta y_2 \\ 2y_1 + 2\beta y_2 & 2\beta y_1 + 6y_2 \end{pmatrix} \begin{pmatrix} \bar{y}_1 \\ \bar{y}_2 \end{pmatrix} p_2 \\ & \geq \rho \sum_{i=1}^2 \left( \|\bar{y}_i\|_{H^{2,1}(Q)}^2 + \|\bar{u}_i\|_{L^2(Q)}^2 \right) \end{aligned}$$

with some  $\rho > 0$ , then  $(y, u)$  is a strict local optimal solution.

**Proof.** The proof follows from the general result in [26].  $\square$

As is usually the case for optimal control problems with quadratic objective functions, second-order sufficient conditions are satisfied whenever the adjoint states  $p_1$  and  $p_2$  are "small", i.e., whenever the desired states and trajectories  $y_{iT}$  and  $y_{id}$  can be approached reasonably well.

**Proposition 7 (Adjoint regularity)** *If the desired terminal states  $y_{iT}$  are in  $H^1(\Omega)$  (or in  $H_0^1(\Omega)$  in the case of Dirichlet boundary conditions), then the adjoint states  $p_i$  are in  $H^{2,1}(Q)$ .*

## 5 Discretization and multigrid solution of $\lambda - \omega$ optimality systems

To validate the effectiveness of the distributed optimal control mechanism analyzed in the previous section, the numerical solution of the optimality system is required. This is a difficult task especially in the regime of turbulent behavior. To achieve this goal, we propose a space-time multigrid approach whose main component is a new robust smoothing iteration suitable for small diffusivity  $\sigma$  required for turbulent evolution. Space-time multigrid schemes were originally proposed in [13] to solve scalar parabolic problems. For a recent contribution in this field see [16].

While this iteration has been developed to solve  $\lambda - \omega$  optimality systems with distributed control, its applicability is not limited to this case. In fact, it can be easily extended to solve other nonlinear multi-species reaction-diffusion optimal control problems. In addition, our approach is also capable of solving boundary control problems after the necessary modifications. In doing so, we have verified that boundary control is unable to influence the chaotic  $\lambda - \omega$  system in regions away from the boundary. This is due to the small diffusivity and the turbulent behavior of the system.

We discuss our multigrid framework considering the  $\lambda - \omega$  optimality system discretized by finite differences and the backward Euler scheme as follows. Let us denote by  $\{\Omega_h\}_{h>0}$  a sequence of uniform grids and assume for simplicity that  $\Omega$  is a square. In the sequel,  $\Omega_h$  is the set of interior mesh-points  $\mathbf{x}_{ij} = (x_{1i}, x_{2j})$ ,  $x_{1i} = (i - 1)h$  and  $x_{2j} = (j - 1)h$ ,  $i, j = 2, \dots, N_{\mathbf{x}} + 1$ . The Laplacian with homogeneous Neumann or Dirichlet boundary conditions is approximated by the common five-point stencil and denoted by  $\Delta_h$ .

For grid functions  $v_h$  and  $w_h$  defined on  $\Omega_h$  we introduce the discrete  $L^2(\Omega)$ -scalar product  $(v_h, w_h)_{L_h^2(\Omega_h)} = h^2 \sum_{\mathbf{x} \in \Omega_h} v_h(\mathbf{x}) w_h(\mathbf{x})$  with associated norm  $|v_h|_0 = (v_h, v_h)_{L_h^2(\Omega_h)}^{1/2}$ . Moreover, let us denote by  $\Delta t = T/N_t$  the time step size and define the space-time grid

$$Q_{h,\Delta t} = \{(\mathbf{x}, t_m) : \mathbf{x} \in \Omega_h, t_m = (m - 1)\Delta t, 1 \leq m \leq N_t + 1\}.$$

On this grid,  $y_h^m$  denotes a grid function at time level  $m$ . The action of the backward and forward time difference operators on such a function is defined by

$$\partial_t^+ y_h^m = \frac{y_h^m - y_h^{m-1}}{\Delta t} \quad \text{and} \quad \partial_t^- y_h^m = \frac{y_h^{m+1} - y_h^m}{\Delta t},$$

respectively; see [2] for details. For grid functions defined on  $Q_{h,\Delta t}$  we use the discrete  $L^2(Q)$ -scalar product with norm  $\|v_{h,\Delta t}\|_0 = (v_{h,\Delta t}, v_{h,\Delta t})_{L^2_{h,\Delta t}(Q_{h,\Delta t})}^{1/2}$  where  $(v_{h,\Delta t}, w_{h,\Delta t})_{L^2_{h,\Delta t}(Q_{h,\Delta t})} = \Delta t h^2 \sum_{(\mathbf{x},t) \in Q_{h,\Delta t}} v_h(\mathbf{x}, t) w_h(\mathbf{x}, t)$ . For convenience, it is assumed that there exist positive constants  $c_1 \leq c_2$  such that  $c_1 h^2 \leq \Delta t \leq c_2 h^2$ . Hence  $h$  can be considered as the only discretization parameter and we write  $v_h$  instead of  $v_{h,\Delta t}$ .

We can now specify the discrete optimal control problem, assuming sufficient regularity of the data,  $y_{iT}$ ,  $y_{id}$ ,  $y_{i0}$ , such that these functions are properly approximated by their values at grid points. For  $\alpha_i, \beta_i \geq 0$  and  $\gamma_i > 0$ , we have

$$\text{Minimize} \quad \sum_{i=1}^2 \left( \frac{\alpha_i}{2} |y_{ih}(\cdot, T) - y_{iT}|_0^2 + \frac{\beta_i}{2} \|y_{ih} - y_{id}\|_0^2 + \frac{\gamma_i}{2} \|u_{ih}\|_0^2 \right)$$

subject to

$$\partial_t^+ \begin{pmatrix} y_1 \\ y_2 \end{pmatrix}_h^m = \begin{bmatrix} 1 - (y_1^2 + y_2^2) & \beta(y_1^2 + y_2^2) \\ -\beta(y_1^2 + y_2^2) & 1 - (y_1^2 + y_2^2) \end{bmatrix}_h \begin{pmatrix} y_1 \\ y_2 \end{pmatrix}_h^m + \sigma \Delta_h \begin{pmatrix} y_1 \\ y_2 \end{pmatrix}_h^m + \begin{pmatrix} u_1 \\ u_2 \end{pmatrix}_h^m.$$

The optimality system related to this problem is found to be

$$\begin{aligned} \partial_t^+ \begin{pmatrix} y_1 \\ y_2 \end{pmatrix}_h^m &= \begin{bmatrix} 1 - (y_1^2 + y_2^2) & \beta(y_1^2 + y_2^2) \\ -\beta(y_1^2 + y_2^2) & 1 - (y_1^2 + y_2^2) \end{bmatrix}_h \begin{pmatrix} y_1 \\ y_2 \end{pmatrix}_h^m + \sigma \Delta_h \begin{pmatrix} y_1 \\ y_2 \end{pmatrix}_h^m \\ &\quad + \begin{pmatrix} u_1 \\ u_2 \end{pmatrix}_h^m, \quad m = 2, \dots, N_t + 1, \end{aligned} \quad (14)$$

$$\begin{aligned} -\partial_t^- \begin{pmatrix} p_1 \\ p_2 \end{pmatrix}_h^m &= \begin{bmatrix} 1 - 3y_1^2 - y_2^2 + 2\beta y_1 y_2 & -3\beta y_1^2 - \beta y_2^2 - 2y_1 y_2 \\ \beta y_1^2 + 3\beta y_2^2 - 2y_1 y_2 & 1 - y_1^2 - 3y_2^2 - 2\beta y_1 y_2 \end{bmatrix}_h \begin{pmatrix} p_1 \\ p_2 \end{pmatrix}_h^m \\ &\quad + \sigma \Delta_h \begin{pmatrix} p_1 \\ p_2 \end{pmatrix}_h^m - \begin{pmatrix} \beta_1(y_1 - y_{1d}) \\ \beta_2(y_2 - y_{2d}) \end{pmatrix}_h^m, \quad m = 1, \dots, N_t. \end{aligned} \quad (15)$$

For  $m = 1, \dots, N_t + 1$  we have

$$\gamma_1 u_{1h}^m - p_{1h}^m = 0 \quad \text{and} \quad \gamma_2 u_{2h}^m - p_{2h}^m = 0, \quad (16)$$

with initial condition at  $t = 0$  and terminal condition at  $t = T$  given by

$$\begin{pmatrix} y_1 \\ y_2 \end{pmatrix}_h^1 = \begin{pmatrix} y_{10} \\ y_{20} \end{pmatrix}_h \quad \text{and} \quad \begin{pmatrix} p_1 \\ p_2 \end{pmatrix}_h^{N_t+1} = - \begin{pmatrix} \alpha_1(y_1 - y_{1T}) \\ \alpha_2(y_2 - y_{2T}) \end{pmatrix}_h^{N_t+1} \quad (17)$$

respectively.

The discrete optimality system (14)–(17) is characterized by two pairs of reaction-diffusion equations. Unconditional stability and  $\mathcal{O}(\Delta t + h^2)$  accuracy of solutions to (14) and (15) can be proved using results in [3].

We comment on the coupling structure between these equations. On the one hand, the state variables are coupled to the adjoint variables through (16) which act as source terms. On the other hand, the coefficients of the adjoint equations as well as the terminal condition depend on the state variables. Moreover the state and adjoint equations have opposite time orientation. All these features are unusual in scientific computing and existing methods often cannot be applied directly to solve (14)–(17) in an efficient way. Also within computational optimization, classical approaches like forward-backward sequential solution do not allow a robust implementation of the time coupling between the state and adjoint variables.

Motivated by the properties and difficulties listed above, a space-time multigrid framework was proposed and analyzed in [2]. In this reference it is shown that considering parabolic optimality systems in the whole space-time domain and using appropriate collective smoothing iterations allow a robust implementation of the coupling between state and adjoint variables. However, the pointwise smoothing considered in [2] becomes less effective as the diffusion coefficient  $\sigma$  tends to be small. In this paper, our aim is to develop a multigrid scheme capable of solving the optimality system (14)–(17) efficiently for a large range of optimization parameters and in particular for small  $\sigma$ . For this purpose we first discuss a new smoothing iteration for our space-time multigrid scheme, described later in this section.

It is well known [35] that in order for an iterative scheme to be efficient for smoothing, it must be applied in the direction of strong coupling of the stencil of the operator. Now, for  $\sigma$  small the coupling in the space direction is weak and therefore pointwise relaxation is not effective in reducing the high-frequency components of the error. To overcome this limitation, block-relaxation of the variables that are strongly connected should be performed. In our case this means solving simultaneously for the pairs of state and adjoint variables along the time-direction at each space point. This type of smoothing belongs to the class of block collective Gauss-Seidel relaxation [35] and is defined in the sequel.

Assume a Gauss-Seidel procedure defined on  $\Omega_h$ . At the space-grid point indexed by  $ij$ , consider the discrete optimality system (14)–(16) for all time steps. For simplicity, we can plug in the optimality conditions (16) into (14) to eliminate the control variables so that four variables at each grid point have to be determined. Thus, corresponding to each spatial grid point  $ij$ , we obtain a block-tridiagonal system in which the off-diagonal blocks arise from the time-derivative stencils. Each block is a  $4 \times 4$  matrix corresponding to the vector of variables  $(y_1, p_1, y_2, p_2)$  at  $ij$  and time level  $m$ . The solution of the tridiagonal system is used to update all variables defined on  $\mathbf{x}_{ij}$  for  $m = 2, \dots, N_t + 1$ . This is one step of our smoothing iteration. Repeating this process at each  $\mathbf{x} \in \Omega_h$  in some order (lexicographic order in our case) defines one smoothing sweep.

Now we discuss this smoothing process in detail. Let us multiply the equations (14) and (15) by  $\Delta t$ . Denote with  $C_m$  and  $E_m$  the left-hand side and right-hand side off-diagonal blocks originating from the  $\partial_t^+$  and the  $\partial_t^-$  stencils, respectively. We have

$$C_m = \begin{bmatrix} 1 & 0 & 0 & 0 \\ 0 & 0 & 0 & 0 \\ 0 & 0 & 1 & 0 \\ 0 & 0 & 0 & 0 \end{bmatrix} \quad \text{and} \quad E_m = \begin{bmatrix} 0 & 0 & 0 & 0 \\ 0 & 1 & 0 & 0 \\ 0 & 0 & 0 & 0 \\ 0 & 0 & 0 & 1 \end{bmatrix}. \quad (18)$$

Also from (14) and (15) we obtain the diagonal block  $D_m$  for  $m = 2, \dots, N_t$ , given by

$$D_m = \begin{bmatrix} -c + \Delta t \lambda & \frac{\Delta t}{\gamma_1} & -\Delta t \omega & 0 \\ -\Delta t \beta_1 & -c + \Delta t g_{11} & 0 & \Delta t g_{12} \\ \Delta t \omega & 0 & -c + \Delta t \lambda & \frac{\Delta t}{\gamma_2} \\ 0 & \Delta t g_{21} & -\Delta t \beta_2 & -c + \Delta t g_{22} \end{bmatrix}, \quad (19)$$

where all functions are evaluated at  $t_m$ ,  $c = 1 + 4 \Delta t \sigma / h^2$ , and  $G = (g_{ij})$  is given by

$$G = \begin{bmatrix} 1 - 3y_1^2 - y_2^2 + 2\beta y_1 y_2 & -3\beta y_1^2 - \beta y_2^2 - 2y_1 y_2 \\ \beta y_1^2 + 3\beta y_2^2 - 2y_1 y_2 & 1 - y_1^2 - 3y_2^2 - 2\beta y_1 y_2 \end{bmatrix}_h^m.$$

Notice that we consider the terms within brackets  $[\ ]$  as frozen during the smoothing step. Clearly, at each time step, the variables neighboring the point  $ij$ , which enter the discretization because of the Laplacian, are taken as constant and contribute to the right-hand side of the system.



3. end.

Notice that block-tridiagonal systems can be solved efficiently with  $\mathcal{O}(N_t)$  effort.

The smoothing properties of this iterative scheme are discussed later in this section, now we complete the present discussion describing FAS multigrid scheme [4] used to solve the  $\lambda - \omega$  optimality system. In general, an initial approximation to the optimal solution will differ from the exact solution because of errors involving high-frequency as well as low-frequency components. In order to solve for all frequency components of the error, the multigrid strategy combines two complementary schemes. The high-frequency components of the error are reduced by smoothing iterations while the low-frequency error components are effectively reduced by a coarse-grid correction method.

To formulate the multigrid solution process, let us consider  $L$  grid levels indexed by  $k = 1, \dots, L$ , where  $k = L$  refers to the finest grid. Any operator and variable defined on level  $k$  is indexed by  $k$ . The mesh of level  $k$  is denoted by  $Q_k = Q_{h_k, \Delta t_k}$  where  $h_k = h_1/2^{k-1}$  and  $\Delta t_k = \Delta t$ , thus we employ semicoarsening in space [16]. Our choice of the semicoarsening strategy is suggested by results of experiments and analysis presented in [2] where superior efficiency and robustness of this method with respect to standard coarsening in the time direction is demonstrated.

The optimality system at level  $k$  with given initial, terminal, and boundary conditions is represented by the following nonlinear equation

$$A_k(w_k) = f_k, \quad (22)$$

where  $w_k = (y_1, p_1, y_2, p_2)_k$ . In case of Neumann boundary conditions, we consider (14)–(15) also on the boundary and use (7a) discretized by second-order centered finite differences to eliminate the (ghost) variables outside of the domain.

The action of one FAS-cycle applied to (22) is expressed in terms of the (non-linear) multigrid iteration operator  $B_k$ . Starting with an initial approximation  $w_k^{(0)}$  the result of one FAS- $(\nu_1, \nu_2)$ -cycle is denoted by  $w_k = B_k(w_k^{(0)}) f_k$ . Let  $S_k$ , denote the smoothing operator defined above.

**Algorithm 9** *Multigrid FAS- $(\nu_1, \nu_2)$ -Cycle.* Set  $B_1(w_1^{(0)}) \approx A_1^{-1}$  (e.g., solve by smoothing). For  $k = 2, \dots, L$  define  $B_k$  in terms of  $B_{k-1}$  as follows.

1. Set the starting approximation  $w_k^{(0)}$ .
2. Pre-smoothing. Define  $w_k^{(l)}$  for  $l = 1, \dots, \nu_1$ , by  $w_k^{(l)} = S_k(w_k^{(l-1)}, f_k)$ .
3. Coarse grid correction. Set  $w_k^{(\nu_1+1)} = w_k^{(\nu_1)} + I_{k-1}^k(w_{k-1} - \hat{I}_k^{k-1}w_k^{(\nu_1)})$  where
 
$$w_{k-1} = B_{k-1}(\hat{I}_k^{k-1}w_k^{(\nu_1)}) \left[ I_k^{k-1}(f_k - A_k(w_k^{(\nu_1)})) + A_{k-1}(\hat{I}_k^{k-1}w_k^{(\nu_1)}) \right].$$
4. Post-smoothing. Define  $w_k^{(l)}$  for  $l = \nu_1 + 2, \dots, \nu_1 + \nu_2 + 1$ , by  $w_k^{(l)} = S_k(w_k^{(l-1)}, f_k)$ .
5. Set  $B_k(w_k^{(0)}) f_k = w_k^{(\nu_1+\nu_2+1)}$ .

In our implementation, we choose  $I_k^{k-1}$  to be the full-weighted restriction operator [35] in space with no averaging in the time direction. The mirrored version of this operator applies also to the boundary points. We choose  $\hat{I}_k^{k-1}$  to be straight injection. The prolongation  $I_{k-1}^k$  is defined by bilinear interpolation in space. No interpolation in time is needed.

Let us discuss further details of Algorithm 9. On the grid of level  $k$ , first the smoothing procedure  $S_k$  is applied  $\nu_1$  times to damp efficiently the high error components. If this is the case, then the grid  $\Omega_{k-1}$  should provide enough resolution for the error of  $w_k$  and hence  $w_{k-1} - \hat{I}_k^{k-1}w_k$  should be a good approximation to this error on the coarse grid. Here  $w_{k-1}$  denotes the solution to the coarse-grid problem  $A_{k-1}(w_{k-1}) = f_{k-1} + \tau_k^{k-1}$  where  $f_{k-1} = I_k^{k-1}f_k$  and  $\tau_k^{k-1}$  is the fine-to-coarse defect correction given by

$$\tau_k^{k-1} = A_{k-1}(\hat{I}_k^{k-1}w_k^{(\nu_1)}) - I_k^{k-1}A_k(w_k^{(\nu_1)}).$$

Once the coarse grid problem is solved, the coarse grid correction follows

$$w_k^{(\nu_1+1)} = w_k^{(\nu_1)} + I_{k-1}^k(w_{k-1} - \hat{I}_k^{k-1}w_k^{(\nu_1)}).$$

The idea of transferring the problem to be solved to a coarser grid is applied along the set of nested meshes. One starts at level  $L$  with, e.g., a zero approximation and applies the smoothing iteration  $\nu_1$  times. Then the problem is transferred to a coarser grid and so on. Once the coarsest grid is reached, one solves the coarsest problem to convergence by applying, as we do, a few steps of the smoothing iteration. The solution obtained on each grid is then used to correct the approximation on the next finer grid. The

coarse-grid correction followed by  $\nu_2$  post-smoothing steps is applied from one grid to the next, down to the finest grid with level  $L$ . The purpose of post-smoothing is to damp possible high-frequency components which may arise from the interpolation process.

We conclude this section investigating the smoothing property of Algorithm 8 depending on  $\sigma$ . Later, we comment on the convergence properties of Algorithm 9. A classical tool for estimating the convergence of multigrid algorithms is local Fourier analysis; see, e.g., [16, 35]. To apply this tool we consider a linearized  $\lambda - \omega$  optimality system consistently with the construction of the smoothing Algorithm 8 on infinite grids.

On these grids, consider the Fourier components  $\phi(\mathbf{j}, \boldsymbol{\theta}) = \mathbf{a} e^{i\mathbf{j} \cdot \boldsymbol{\theta}}$  where  $\mathbf{a} = (1, 1, 1, 1)^\top$ ,  $i$  is the imaginary unit,  $\mathbf{j} = (j_1, j_2, j_t) \in \mathbb{Z} \times \mathbb{Z} \times \mathbb{Z}$ ,  $\boldsymbol{\theta} = (\theta_1, \theta_2, \theta_t) \in [-\pi, \pi]^3$ , and  $\mathbf{j} \cdot \boldsymbol{\theta} = j_1\theta_1 + j_2\theta_2 + j_t\theta_t$ . Here, the sub-indices 1 and 2 refer to the space coordinates. A grid point on the infinite grid is  $(x_1, x_2, t) = (j_1h, j_2h, j_t\Delta t)$ .

In correspondence with semicoarsening in space, one defines

$$\phi \text{ low frequencies (LF)} \iff (\theta_1, \theta_2) \in [-\frac{\pi}{2}, \frac{\pi}{2}]^2, \quad \theta_t \in [-\pi, \pi],$$

$$\phi \text{ high frequencies (HF)} \iff (\theta_1, \theta_2) \in [-\pi, \pi]^2 \setminus [-\frac{\pi}{2}, \frac{\pi}{2}]^2, \quad \theta_t \in [-\pi, \pi].$$

Now assume the following decomposition of the error  $\sum_{\boldsymbol{\theta}} W_{\boldsymbol{\theta}} \phi(\mathbf{j}, \boldsymbol{\theta})$  where the  $W_{\boldsymbol{\theta}}$  represent the Fourier coefficients. The action of one smoothing step on this error can be expressed as  $W_{\boldsymbol{\theta}}^{(1)} = \hat{S}(\boldsymbol{\theta}) W_{\boldsymbol{\theta}}^{(0)}$  where  $\hat{S}(\boldsymbol{\theta})$  is the Fourier symbol [35] of the smoothing operator. To determine  $\hat{S}(\boldsymbol{\theta})$ , recall that the functions  $\phi(\mathbf{j}, \boldsymbol{\theta})$  are eigenfunctions of any discrete operator described by a difference stencil on a infinite grid. Therefore we formally have  $S_h \phi(\mathbf{j}, \boldsymbol{\theta}) = \hat{S}(\boldsymbol{\theta}) \phi(\mathbf{j}, \boldsymbol{\theta})$ , that is, the symbol of  $S_h$  is its (formal) eigenvalue [35]. Now consider one step of our smoothing iteration at  $(j_1, j_2)$  which results in zero residuals after update. In terms of Fourier modes this corresponds, for each Fourier component, to the following equation (for clarity, multiply by  $e^{i(j_1\theta_1 + j_2\theta_2 + j_t\theta_t)}$ )

$$(C e^{-i\theta_t} + D + E e^{i\theta_t} + \tilde{I} e^{-i\theta_1} + \tilde{I} e^{-i\theta_2}) W_{\boldsymbol{\theta}}^{(1)} = -(\tilde{I} e^{i\theta_1} + \tilde{I} e^{i\theta_2}) W_{\boldsymbol{\theta}}^{(0)},$$

where  $D$ ,  $C$ , and  $E$  are given in (19) and (18), respectively. Notice that  $D$  represents the center of the stencil of the optimality system, and  $C$  and  $E$  the sides of the stencil in the time direction with  $-\Delta t$  and  $+\Delta t$  shift. The term  $\tilde{I} = (\Delta t \sigma / h^2) I$ , where  $I$  is the  $4 \times 4$  identity matrix, allows to

represent the contribution to the stencil in the space direction due to the Laplacian. Here we assume updating in lexicographic order, in the sense that the variables on the grid points  $(j_1 - 1, j_2)$  and  $(j_1, j_2 - 1)$  have been already updated and thus they multiply the Fourier coefficient  $W_{\boldsymbol{\theta}}^{(1)}$ . On the other hand, the variables on  $(j_1 + 1, j_2)$  and  $(j_1, j_2 + 1)$  remain to be updated and thus they multiply  $W_{\boldsymbol{\theta}}^{(0)}$ . It should be now clear that the solution of the equation above provides the symbol of the smoothing iteration as follows

$$\hat{\mathcal{S}}(\boldsymbol{\theta}) = -(C e^{-i\theta_t} + D + E e^{i\theta_t} + \tilde{I} e^{-i\theta_1} + \tilde{I} e^{-i\theta_2})^{-1} (\tilde{I} e^{i\theta_1} + \tilde{I} e^{i\theta_2}). \quad (23)$$

The knowledge of the symbol of the smoothing operator allows to quantitatively determine the ability of the iterative scheme in reducing the high-frequency components of the error. This gives the following smoothing factor estimate

$$\mu_{\text{est}} = \sup \{ |r(\hat{\mathcal{S}}(\boldsymbol{\theta}))| : \boldsymbol{\theta} \text{ high frequencies} \},$$

where  $r$  denotes the spectral radius. Since  $\hat{\mathcal{S}}$  is a  $4 \times 4$  matrix it is possible to directly determine  $\mu_{\text{est}}$  for a large choice of parameters. With  $\mu_{\text{est}}$  known and assuming an ideal coarse-grid correction that annihilates the LF error components and leaves the HF error components unchanged, an estimate of the multigrid convergence factor is given by  $\rho_{\text{est}} = \mu_{\text{est}}^{\nu_1 + \nu_2}$ .

Table 1: Smoothing factors depending on  $\sigma$ .  $\beta = 1$ ,  $s^2 = 0.5$ ,  $\Delta t = 1/64$ ,  $h = 1/128$ ,  $\gamma_i = 10^{-3}$ ,  $i = 1, 2$ ;  $\nu_1 = \nu_2 = 2$ .

Case $\alpha_i = 0$ , $\beta_i = 1$ , $i = 1, 2$ (tracking type)					
$\sigma$	$10^{-4}$	$10^{-3}$	$10^{-2}$	$10^{-1}$	1
$\mu_{\text{est}}$	0.108	0.498	0.455	0.448	0.447
$\rho_{\text{est}}$	0.0001	0.0615	0.0429	0.0403	0.0399
Case $\alpha_i = 1$ , $\beta_i = 0$ , $i = 1, 2$ (terminal obs.)					
$\sigma$	$10^{-4}$	$10^{-3}$	$10^{-2}$	$10^{-1}$	1
$\mu_{\text{est}}$	0.385	0.470	0.449	0.447	0.447
$\rho_{\text{est}}$	0.0220	0.0488	0.0406	0.0399	0.0399

In Table 1, we report results for the cases  $\alpha_i = 0$ ,  $\beta_i = 1$  and  $\alpha_i = 1$ ,  $\beta_i = 0$ . In both cases, the smoothing factors have been estimated using (23) with (18) and

$$D = \begin{bmatrix} -c + \Delta t \lambda & \frac{\Delta t}{\gamma_1} & -\Delta t \omega & 0 \\ -\Delta t \beta_1 & -c + \Delta t \lambda & 0 & \Delta t \omega \\ \Delta t \omega & 0 & -c + \Delta t \lambda & \frac{\Delta t}{\gamma_2} \\ 0 & \Delta t \omega & -\Delta t \beta_2 & -c + \Delta t \lambda \end{bmatrix}$$

corresponding to the  $\lambda - \omega$  system with frozen  $\lambda(s)$  and  $\omega(s)$ ,  $\beta = 1$ ,  $s^2 = y_1^2 + y_2^2 = 0.5$ ,  $y_1 = y_2$ . Comparing the estimates  $\rho_{\text{est}}$  in Table 1 with the observed rates in Tables 2–5 of Section 6, we notice that in the case of terminal observation, the estimated convergence rates are rather optimistic, while in the case of tracking type, the estimates are much more accurate. Similar results are obtained with different values of  $\beta$  and values of  $\lambda(s)$  and  $\omega(s)$ .

## 6 Numerical experiments

Results of experiments are reported in this section to validate the effectiveness of distributed optimal control of  $\lambda - \omega$  systems in the turbulent regime. We require that the the control drives the system from a fully evolved chaotic state to an ordered one and discuss the convergence properties of the multigrid method described above.

In the experiments, we use the multigrid scheme given by Algorithm 9 with two pre- and post-smoothing sweeps given by Algorithm 8. The coarsest space grid consists of four intervals in each spatial direction. We report the measured multigrid convergence factor  $\rho$ , defined as the “asymptotic” mean-value of the ratio of the norm of the dynamic residuals given by  $\|r_y\|_0 + \|r_p\|_0$  resulting from two successive multigrid cycles. The tracking ability inherent in the problem at hand is expressed in terms of values of the tracking functionals,  $\|y_i - y_{id}\|_0$  and  $|y_i - y_{iT}|_0$ , respectively.

We choose the domain  $\Omega = (0, 1) \times (0, 1)$ . The initial condition of the optimal control problem is defined as the solution of the freely evolving lambda-omega system with  $\beta = 2$  at  $t_0 = 200$ . The initial conditions for this setup problem are given by

$$y_1 = (x_1 - 1/2)/10 \text{ and } y_2 = (-x_2 + 1/2)/20.$$

The resulting  $y_{10}$  and  $y_{20}$  functions represent disordered states; see Figure 1 (right). We consider the optimal control problem in the time interval  $[0, 1]$  where  $t = 0$  corresponds to  $t_0$  given above. The desired state trajectories are given by

$$y_{1d}(\mathbf{x}, t) = \sin(2\pi r) \sin(\pi x_1) \sin(\pi x_2) \cos(4\pi t),$$

and

$$y_{2d}(\mathbf{x}, t) = \cos(2\pi r) \sin(\pi x_1) \sin(\pi x_2) \sin(4\pi t),$$

where  $r = \sqrt{(x_1 - 1/2)^2 + (x_2 - 1/2)^2}$ . The desired terminal states are given by  $y_{iT}(\mathbf{x}) = y_{id}(\mathbf{x}, T)$ ,  $i = 1, 2$ .

The first series of experiments results from the setting  $\alpha_i = 0$  and  $\beta_i = 1$ ,  $i = 1, 2$ , corresponding to a tracking-type problem. In Table 2, we observe fast convergence almost independent of the mesh size. Notice that as  $\gamma_i$  tends to be small the convergence speed of the multigrid algorithm improves. This is a typical robustness feature of the class of space-time multigrid scheme considered here; see also [2]. Further numerical experiments show that the multigrid iteration is not sensitive to the value of the reaction parameter  $\beta$ . These facts are in agreement with results of local Fourier analysis. Notice in Table 2 that, as the value of  $\gamma$  increases, naturally larger values of the tracking errors are obtained. Similar results are reported in Table 3 in case of Neumann boundary conditions.

Table 2: Convergence and tracking properties depending on  $\gamma_1 = \gamma_2 = \gamma$ ;  $\alpha_i = 0$  and  $\beta_i = 1$ ,  $i = 1, 2$  (tracking type);  $\beta = 2$ ,  $\sigma = 10^{-4}$ . Dirichlet boundary conditions.

$\gamma$	$N_{\mathbf{x}} \times N_{\mathbf{x}} \times N_t$	$\rho$	$\ y_1 - y_{1d}\ _0$	$\ y_2 - y_{2d}\ _0$
$10^{-1}$	$64 \times 64 \times 50$	0.002	$3.37 \cdot 10^{-1}$	$2.86 \cdot 10^{-1}$
$10^{-3}$	$64 \times 64 \times 50$	0.001	$7.45 \cdot 10^{-2}$	$5.90 \cdot 10^{-2}$
$10^{-5}$	$64 \times 64 \times 50$	$< 0.001$	$2.34 \cdot 10^{-3}$	$1.93 \cdot 10^{-3}$
$10^{-1}$	$128 \times 128 \times 100$	0.07	$3.49 \cdot 10^{-1}$	$2.82 \cdot 10^{-1}$
$10^{-3}$	$128 \times 128 \times 100$	$< 0.001$	$8.66 \cdot 10^{-2}$	$6.52 \cdot 10^{-2}$
$10^{-5}$	$128 \times 128 \times 100$	$< 0.001$	$5.88 \cdot 10^{-3}$	$4.55 \cdot 10^{-3}$

The second series of experiments corresponds to the setting  $\alpha_i = 1$  and  $\beta_i = 0$ ,  $i = 1, 2$  (observation of the terminal state), and are reported in Table 4 and 5. With this setting a much more difficult problem results. Nevertheless the proposed multigrid scheme provides efficient and robust solution since only a weak dependence of the convergence factor on the value of the weights  $\gamma_i$  and on the mesh size is observed. Compared with the previous set of experiments, we obtain less competitive convergence factors which however tend to improve as the  $\gamma_i$  become smaller.

The results reported in Tables 2–5 show that in all cases the controlled system comes close to the desired state. It appears that the efficiency of the present multigrid scheme is related to the ability of the control to drive the system from a disordered state to an ordered one. For this purpose, the case of final observation seems to require sufficiently small  $\gamma_i$ . In Figure 2, snapshots of controlled and uncontrolled state variables for the more challenging case of final observation are depicted. Observe that, in the

Table 3: Convergence and tracking properties depending on  $\gamma_1 = \gamma_2 = \gamma$ ;  $\alpha_i = 0$  and  $\beta_i = 1$ ,  $i = 1, 2$  (tracking type);  $\beta = 2$ ,  $\sigma = 10^{-4}$ . Neumann boundary conditions.

$\gamma$	$N_{\mathbf{x}} \times N_{\mathbf{x}} \times N_t$	$\rho$	$\ y_1 - y_{1d}\ _0$	$\ y_2 - y_{2d}\ _0$
$10^{-1}$	$64 \times 64 \times 50$	0.002	$3.47 \cdot 10^{-1}$	$2.89 \cdot 10^{-1}$
$10^{-3}$	$64 \times 64 \times 50$	$< 0.001$	$7.66 \cdot 10^{-2}$	$6.03 \cdot 10^{-2}$
$10^{-5}$	$64 \times 64 \times 50$	$< 0.001$	$2.40 \cdot 10^{-3}$	$2.00 \cdot 10^{-3}$
$10^{-1}$	$128 \times 128 \times 100$	0.09	$3.54 \cdot 10^{-1}$	$2.97 \cdot 10^{-1}$
$10^{-3}$	$128 \times 128 \times 100$	$< 0.001$	$8.58 \cdot 10^{-2}$	$7.00 \cdot 10^{-2}$
$10^{-5}$	$128 \times 128 \times 100$	$< 0.001$	$5.81 \cdot 10^{-3}$	$4.95 \cdot 10^{-3}$

Table 4: Convergence and tracking properties depending on  $\gamma_1 = \gamma_2 = \gamma$ ;  $\alpha_i = 1$  and  $\beta_i = 0$ ,  $i = 1, 2$  (terminal observation);  $\beta = 2$ ,  $\sigma = 10^{-4}$ . Dirichlet boundary conditions.

$\gamma$	$N_{\mathbf{x}} \times N_{\mathbf{x}} \times N_t$	$\rho$	$ y_1 - y_{1T} _0$	$ y_2 - y_{2T} _0$
$10^{-1}$	$64 \times 64 \times 50$	0.64	$5.77 \cdot 10^{-2}$	$5.17 \cdot 10^{-2}$
$10^{-3}$	$64 \times 64 \times 50$	0.67	$6.36 \cdot 10^{-4}$	$5.49 \cdot 10^{-4}$
$10^{-5}$	$64 \times 64 \times 50$	0.68	$6.36 \cdot 10^{-6}$	$5.49 \cdot 10^{-6}$
$10^{-1}$	$128 \times 128 \times 100$	0.78	$5.81 \cdot 10^{-2}$	$5.51 \cdot 10^{-2}$
$10^{-3}$	$128 \times 128 \times 100$	0.67	$6.47 \cdot 10^{-4}$	$5.80 \cdot 10^{-4}$
$10^{-5}$	$128 \times 128 \times 100$	0.40	$6.48 \cdot 10^{-6}$	$5.80 \cdot 10^{-6}$
$10^{-7}$	$128 \times 128 \times 100$	0.35	$6.48 \cdot 10^{-8}$	$5.80 \cdot 10^{-8}$

Table 5: Convergence and tracking properties depending on  $\gamma_1 = \gamma_2 = \gamma$ ;  $\alpha_i = 1$  and  $\beta_i = 0$ ,  $i = 1, 2$  (terminal observation);  $\beta = 2$ ,  $\sigma = 10^{-4}$ . Neumann boundary conditions.

$\gamma$	$N_{\mathbf{x}} \times N_{\mathbf{x}} \times N_t$	$\rho$	$ y_1 - y_{1T} _0$	$ y_2 - y_{2T} _0$
$10^{-1}$	$64 \times 64 \times 50$	0.95	$5.89 \cdot 10^{-2}$	$5.40 \cdot 10^{-2}$
$10^{-3}$	$64 \times 64 \times 50$	0.54	$6.50 \cdot 10^{-4}$	$5.72 \cdot 10^{-4}$
$10^{-5}$	$64 \times 64 \times 50$	0.38	$6.51 \cdot 10^{-6}$	$5.73 \cdot 10^{-6}$
$10^{-7}$	$64 \times 64 \times 50$	0.38	$6.51 \cdot 10^{-8}$	$5.73 \cdot 10^{-8}$
$10^{-1}$	$128 \times 128 \times 100$	0.98	$5.88 \cdot 10^{-2}$	$5.50 \cdot 10^{-2}$
$10^{-3}$	$128 \times 128 \times 100$	0.66	$6.48 \cdot 10^{-4}$	$5.82 \cdot 10^{-4}$
$10^{-5}$	$128 \times 128 \times 100$	0.62	$6.49 \cdot 10^{-6}$	$5.82 \cdot 10^{-6}$
$10^{-7}$	$128 \times 128 \times 100$	0.44	$6.49 \cdot 10^{-8}$	$5.82 \cdot 10^{-8}$

time interval considered, the evolution of the free state is relatively slow. By taking larger time intervals, the control in the case of final observation becomes less effective. Correspondingly the multigrid convergence factor worsens. In our opinion this fact results from a weakening of the coupling

between observation of the terminal state and control for large time distances especially due to the oscillatory character of the governing equations. This problem deserves further investigation.

## 7 Conclusions

The formulation, analysis, and numerical solution of distributed optimal control problems governed by lambda-omega systems was presented. A new proof of existence of solutions with Dirichlet and Neumann boundary conditions was given. Then a class of distributed optimal control problems was formulated and existence of global optimal solutions was proved. To characterize these solutions, first- and second-order optimality conditions were given.

To investigate the ability of distributed control to drive lambda-omega systems from a chaotic to a ordered state, a space-time multigrid method was developed based on a block collective smoothing scheme. Convergence properties of the resulting solution process were discussed and results of numerical experiments were reported to validate the optimal control formulation.

## A Proofs

### A.1 Proof of Proposition 1

**Proof.** The proof of the first assertion can be carried out along the lines of [12, Lemma 2.3] using the theory of linear partial differential equations. It follows that

$$\begin{aligned} & \|v_1\|_{H^{2,1}(Q)} + \|v_2\|_{H^{2,1}(Q)} \\ & \leq c (\|y_{10}\|_{H^1(\Omega)} + \|y_{20}\|_{H^1(\Omega)} + \|u_1\|_{L^2(Q)} + \|u_2\|_{L^2(Q)}), \end{aligned} \quad (24)$$

where  $c$  is a polynomial in  $\|y_1\|_{H^{2,1}(Q)}$  and  $\|y_2\|_{H^{2,1}(Q)}$ . In the case of Dirichlet boundary values, the compatibility relations  $y_{i0}|_{\partial\Omega} = 0$ , i.e.,  $y_{i0} \in H_0^1(\Omega)$  have to be verified [22].

For the rest of the proof, we elaborate on the case of homogeneous Neumann boundary conditions. The case of Dirichlet boundary conditions proceeds exactly alike. In order to show that  $T$  is compact, let  $\{y_i^n\}$  be weakly convergent sequences in  $H^{2,1}(Q)$ , i.e.,  $y_i^n \rightharpoonup y_i$  in  $H^{2,1}(Q)$ . Let  $v^n$  denote

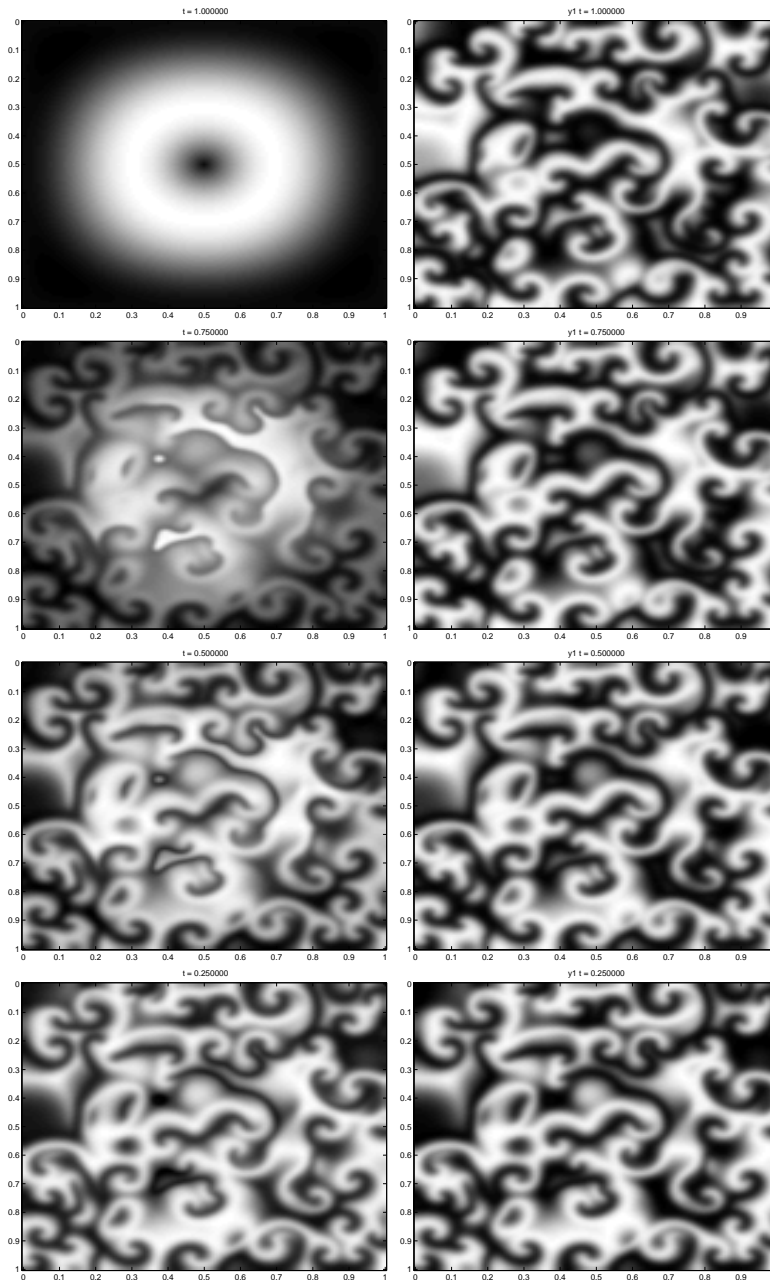


Figure 2: Evolution of optimally controlled (left) and of uncontrolled solution (right)  $y_1$ ;  $\gamma_1 = \gamma_2 = 10^{-5}$ ,  $\alpha_i = 1$  and  $\beta_i = 0$ ,  $i = 1, 2$ ;  $\beta = 2$ ,  $\sigma = 10^{-4}$ , mesh  $128 \times 128 \times 100$ . Neumann boundary conditions.

the solution of (9) with data  $y^n$ , i.e.,  $v^n = Ty^n$ . In view of the a priori bound (24),  $\{v_i^n\}$  is bounded in  $H^{2,1}(Q)$ , since  $\{y_i^n\}$  is bounded in  $H^{2,1}(Q)$ . Therefore, we can extract a subsequence, still denoted by  $\{v_i^n\}$ , such that  $v_i^n \rightharpoonup v_i$  in  $H^{2,1}(Q)$ . For convenience, let us abbreviate

$$A(y) := \begin{bmatrix} 1 - (y_1^2 + y_2^2) & \beta(y_1^2 + y_2^2) \\ -\beta(y_1^2 + y_2^2) & 1 - (y_1^2 + y_2^2) \end{bmatrix}.$$

We note that, for instance,

$$\|(y_1^n)^2 v_1^n - (y_1)^2 v_1\|_{L^2(Q)} \leq \|(y_1^n)^2 [v_1^n - v_1]\|_{L^2(Q)} + \|[(y_1^n)^2 - (y_1)^2] v_1\|_{L^2(Q)}$$

and

$$\begin{aligned} \|(y_1^n)^2 [v_1^n - v_1]\|_{L^2(Q)} &\leq \|y_1^n\|_{L^8(Q)}^2 \cdot \|v_1^n - v_1\|_{L^4(Q)} \\ \|[(y_1^n)^2 - (y_1)^2] v_1\|_{L^2(Q)} &\leq \|y_1^n - y_1\|_{L^8(Q)} \cdot \|y_1^n + y_1\|_{L^8(Q)} \cdot \|v_1\|_{L^4(Q)}. \end{aligned}$$

In view of the compactness of the embedding  $H^{2,1}(Q) \hookrightarrow L^p(Q)$  ( $1 \leq p < \infty$ ), and using similar arguments for the remaining terms, we conclude that  $A(y^n) v^n \rightarrow A(y) v$  strongly in  $[L^2(Q)]^2$ . Using the embedding  $H^{2,1}(Q) \hookrightarrow C([0, T]; H^1)$ , the space of continuous functions with values in  $H^1(\Omega)$ , one infers that  $v$  meets the initial conditions  $(y_{10}, y_{20})$ . Hence the difference  $v^n - v$  satisfies

$$\frac{\partial}{\partial t}(v^n - v) = \sigma \Delta(v^n - v) + A(y^n) v^n - A(y) v$$

with zero initial and boundary conditions, and from a standard a priori estimate we conclude that  $v^n \rightarrow v$  strongly in  $[H^{2,1}(Q)]^2$ . This shows that the nonlinear map  $T$  is compact from  $[H^{2,1}(Q)]^2$  to  $[H^{2,1}(Q)]^2$ .

To conclude the proof, let  $s \in [0, 1]$  be arbitrary, and let  $y \in [H^{2,1}(Q)]^2$  satisfy  $y = sTy$ . We use a bootstrapping argument to derive upper bounds for  $y$ , independent of  $s$ , in the spaces  $L^\infty(0, T; L^2)$ ,  $L^2(0, T; H^1)$ ,  $L^\infty(0, T; H^1)$ , and finally  $H^{2,1}(Q)$ : To keep the expressions shorter, we write  $y_i$  instead of  $y_i(\cdot, t)$ . In the sequel,  $c$  and  $\tilde{c}$  denote generic positive constants and have different meanings in different locations.

We multiply the first and second equations in (6) by  $y_1$  and  $y_2$  and integrate over  $\Omega$ . From integration by parts and Young's inequality we obtain

$$\begin{aligned} &\frac{d}{dt} \|y_1\|_{L^2(\Omega)}^2 + \frac{d}{dt} \|y_2\|_{L^2(\Omega)}^2 + \sigma \|y_1\|_{H^1(\Omega)}^2 + \sigma \|y_2\|_{H^1(\Omega)}^2 \\ &\leq (1 + \sigma) \|y_1\|_{L^2(\Omega)}^2 + (1 + \sigma) \|y_2\|_{L^2(\Omega)}^2 + \frac{1}{2\sigma} \|u_1\|_{L^2(\Omega)}^2 + \frac{1}{2\sigma} \|u_2\|_{L^2(\Omega)}^2, \end{aligned}$$

independent of  $s$ . From Gronwall's inequality [5, Lemma 18.1.i], neglecting the terms  $\sigma \|y_i\|_{H^1(\Omega)}^2$ , we infer that  $y_i$  is bounded in  $L^\infty(0, T; L^2)$  and the bound depends only on the data  $y_{i0}$  and  $u_i$ . Integrating the above inequality over  $[0, T]$ , we derive the same type of bound in  $L^2(0, T; H^1)$ .

In order to pass to the higher order norms, we multiply the first and second equations in (6) by  $-\Delta y_i$  and integrate again over  $\Omega$ . We obtain, similarly as above,

$$\begin{aligned} & \frac{d}{dt} \|\nabla y_1\|_{[L^2(\Omega)]^2}^2 + \frac{d}{dt} \|\nabla y_2\|_{[L^2(\Omega)]^2}^2 + \sigma \|\Delta y_1\|_{L^2(\Omega)}^2 + \sigma \|\Delta y_2\|_{L^2(\Omega)}^2 \\ & \leq \|y_1^2 + y_2^2\|_{L^2(\Omega)}^2 + \|\nabla y_1\|_{[L^2(\Omega)]^2}^2 + \|\nabla y_2\|_{[L^2(\Omega)]^2}^2 + \frac{1}{2\sigma} \|u_1\|_{L^2(\Omega)}^2 + \frac{1}{2\sigma} \|u_2\|_{L^2(\Omega)}^2. \end{aligned}$$

From interpolation theory in Banach spaces, one infers (cf. [34]) that

$$[L^\infty(0, T; L^2), L^2(0, T; H^1)]_\theta = L^{2/\theta}(0, T; H^\theta)$$

and in particular

$$[L^\infty(0, T; L^2), L^2(0, T; H^1)]_{1/2} = L^4(0, T; H^{1/2}).$$

The interpolation inequality  $\|y\|_{[X, Y]_\theta} \leq c_\theta \|y\|_X^{1-\theta} \cdot \|y\|_Y^\theta$  now yields

$$\|y\|_{L^4(0, T; H^{1/2})}^2 \leq c \|y\|_{L^\infty(0, T; L^2)} \cdot \|y\|_{L^2(0, T; H^1)}.$$

Using Hölder's inequality and the embedding  $H^{1/2}(\Omega) \hookrightarrow L^4(\Omega)$  [1], we finally arrive at

$$\|y_i^2\|_{L^2(Q)}^2 \leq \|y_i\|_{L^4(Q)}^4 \leq \tilde{c} \|y\|_{L^4(0, T; H^{1/2})}^4 \leq c \|y_i\|_{L^\infty(0, T; L^2)}^2 \cdot \|y_i\|_{L^2(0, T; H^1)}^2.$$

We now deduce from Gronwall's inequality, neglecting the terms  $\sigma \|\Delta y_i\|_{L^2(\Omega)}$ , that  $y_i$  is bounded in the norm of  $L^\infty(0, T; H^1)$  by a constant which depends only on the data  $y_{i0}$  and  $u_i$ , not on  $s$ . To pass on to the norm of  $H^{2,1}(Q)$ , we are now in the position to apply an a priori bound directly to (6), where the nonlinear parts play the role of source terms. We obtain

$$\begin{aligned} & \|y_1\|_{H^{2,1}(Q)} + \|y_2\|_{H^{2,1}(Q)} \\ & \leq c (\|y_{10}\|_{H^1(\Omega)} + \|y_{20}\|_{H^1(\Omega)} + \|u_1\|_{L^2(Q)} + \|u_2\|_{L^2(Q)}) \\ & \quad + c(1 + \beta) (\|y_1^3 + y_1 y_2^2\|_{L^2(Q)} + \|y_1^2 y_2 + y_2^3\|_{L^2(Q)}), \end{aligned} \quad (25)$$

where in view of  $\|y_i y_j^2\|_{L^2(Q)} \leq \|y_i\|_{L^6(Q)} \cdot \|y_j\|_{L^6(Q)} \cdot \|y_j\|_{L^6(Q)}$  and the embedding  $L^\infty(0, T; H^1) \hookrightarrow L^6(Q)$ , the terms on the right hand side are bounded by a constant which depends only on the data  $y_{i0}$  and  $u_i$ , not on  $s$ .  $\square$

## A.2 Proof of Theorem 2

**Proof.** The existence part follows from the Leray-Schauder Theorem. We obtain the a priori bound (10) from (25), plugging in the previous estimates for the bounds in  $L^\infty(0, T; H^1)$ ,  $L^2(0, T; H^1)$  and  $L^\infty(0, T; L^2)$ .

In order to show uniqueness, assume that  $(y_1, y_2)$  and  $(\bar{y}_1, \bar{y}_2)$  are two solutions of (6)–(8), and let  $w = y - \bar{y}$  be their difference. Then one can show that  $w$  satisfies

$$\begin{aligned} \frac{\partial}{\partial t} \begin{pmatrix} w_1 \\ w_2 \end{pmatrix} &= \begin{bmatrix} 1 - \frac{3}{2}(y_1^2 + \bar{y}_1^2) - \bar{y}_2^2 + 2\beta y_1 \bar{y}_2 & -2y_1 y_2 + \beta y_1^2 + \frac{3}{2}\beta(y_2^2 + \bar{y}_2^2) \\ -\frac{3}{2}\beta(y_1^2 + \bar{y}_1^2) - \beta \bar{y}_2 - 2y_1 \bar{y}_2 & 1 - 2\beta y_1 y_2 - y_1^2 - \frac{3}{2}(y_2^2 + \bar{y}_2^2) \end{bmatrix} \begin{pmatrix} w_1 \\ w_2 \end{pmatrix} \\ &+ \begin{bmatrix} -\beta \bar{y}_2 & y_1 \\ \bar{y}_2 & \beta y_1 \end{bmatrix} \begin{pmatrix} w_1^2 \\ w_2^2 \end{pmatrix} + \begin{bmatrix} \frac{1}{2} & -\frac{1}{2}\beta \\ \frac{1}{2}\beta & \frac{1}{2} \end{bmatrix} \begin{pmatrix} w_1^3 \\ w_2^3 \end{pmatrix} + \sigma \Delta \begin{pmatrix} w_1 \\ w_2 \end{pmatrix}, \end{aligned} \quad (26)$$

with homogeneous Neumann or Dirichlet boundary conditions and zero initial conditions. As before, we multiply (26) by  $w_1(\cdot, t)$  and  $w_2(\cdot, t)$ , respectively, and integrate over  $\Omega$ . Some of the terms of the right hand side have negative sign. The remaining terms are estimated according to the following example:

$$\begin{aligned} \int_{\Omega} y_1 y_2 w_1 w_2 &\leq \|y_1 y_2\|_{L^\infty(\Omega)} \cdot \|w_1\|_{L^2(\Omega)} \cdot \|w_2\|_{L^2(\Omega)} \\ &\leq \frac{1}{2} \|y_1 y_2\|_{L^\infty(\Omega)} \cdot \left( \|w_1\|_{L^2(\Omega)}^2 + \|w_2\|_{L^2(\Omega)}^2 \right) \\ \int_{\Omega} y_1 w_1^2 w_2 &\leq \|y_1 w_2\|_{L^\infty(\Omega)} \cdot \|w_1\|_{L^2(\Omega)}^2. \end{aligned}$$

Clearly, the terms  $\|y_1 y_2\|_{L^\infty(\Omega)}$  and  $\|y_1 w_2\|_{L^\infty(\Omega)}$  are elements of  $L^1(0, T)$ . Hence, we obtain an estimate

$$\frac{d}{dt} \|w_1\|_{L^2(\Omega)}^2 + \frac{d}{dt} \|w_2\|_{L^2(\Omega)}^2 \leq \chi(t) \left( \|w_1\|_{L^2(\Omega)}^2 + \|w_2\|_{L^2(\Omega)}^2 \right)$$

with a function  $\chi \in L^1(0, T)$ . Using Gronwall's lemma, we find that in view of  $\|w_i(\cdot, 0)\|_{L^2(\Omega)} = 0$ ,  $\|w_i\|_{L^2(\Omega)}$  vanishes for all  $t \in [0, T]$ , from where the uniqueness part in Theorem 2 follows.  $\square$

## References

- [1] R. ADAMS, *Sobolev Spaces*, Academic Press, New York, 1975

- [2] A. BORZÌ, *Multigrid methods for parabolic distributed optimal control problems*, J. Comp. Appl. Math., 157 (2003), pp. 365-382.
- [3] A. BORZÌ, *Solution of lambda-omega systems: Theta-schemes and multigrid methods*, Numer. Math., 98(4) (2004), pp. 581-606.
- [4] A. BRANDT, *Multi-level adaptive solutions to boundary-value problems*, Mathematics of Computation, 31 (1977), pp. 333-390.
- [5] L. CESARI, *Optimization: Theory and Applications*, Springer, New York, 1983.
- [6] M. CROSS AND P. HOHENBERG, *Pattern formation outside of equilibrium*, Rev. Mod. Phys. 65, (1993), pp. 851-1112.
- [7] E.D. DAHLBERG AND J.G. ZHU, *Micromagnetic microscopy and modeling*, Physics Today, April 48 (1995), p. 34.
- [8] R. DAUTRAY, J. L. LIONS, *Mathematical Analysis and Numerical Methods for Science and Technology*, Volume 5, Springer, Berlin, 2000
- [9] K. DEIMLING, *Nonlinear Functional Analysis*, Springer, Berlin, 1985.
- [10] A. DUFFY, K. BRITTON, AND J. MURRAY, *Spiral wave solutions of practical reaction-diffusion systems*, SIAM J. Appl. Math, 39(1) (1980), pp. 8-13.
- [11] D. GILBARG, N.S. TRUDINGER, *Elliptic Differential Equations of Second Order*, Springer, Berlin, 1977
- [12] R. GRIESSE, *Parametric sensitivity analysis in optimal control of a reaction diffusion system - Part I: Solution differentiability*, Numerical Functional Analysis and Optimization, 25(1-2) (2004), pp. 93-117.
- [13] W. HACKBUSCH, *Parabolic multigrid methods*, In R. Glowinski and J.-L. Lions, Computing Methods in Applied Sciences and Engineering VI, North-Holland, Amsterdam, 1984.
- [14] A. HAGBERG, E. MERON, I. RUBINSTEIN, AND B. ZALTZMAN, *Controlling domain patterns far from equilibrium*, Phys. Rev. Lett., 76 (1996), pp. 427-430.
- [15] M. HEINKENSCHLOSS AND F. TRÖLTZSCH, *Analysis of the Lagrange-SQP-Newton method for the control of a phase-field equation*, Control Cybernet., 28(2) (1999), pp. 177-211.

- [16] G. HORTON AND S. VANDEWALLE, *A space-time multigrid method for parabolic partial differential equations*, SIAM J. Sci. Comput., 16(4) (1995), pp. 848–864.
- [17] K. ITO AND K. KUNISCH, *Optimal control of the solid fuel ignition model with  $H^1$ -cost*, SIAM J. Control Optim., 40 (2002), pp. 1455–1472.
- [18] A. KAUFFMANN, *Optimal Control of the Solid Fuel Ignition Model*, Ph.D. thesis, Technische Universität Berlin, 1998.
- [19] Y. KURAMOTO, *Chemical Oscillations, Waves, and Turbulence*, Springer-Verlag, 1984.
- [20] Y. KURAMOTO AND S. KOGA, *Turbulized rotating chemical waves*, Prog. Theor. Phys., 66(3) (1981), pp. 1081–1085.
- [21] C.D. LEVERMORE AND M. OLIVER, *The complex Ginzburg-Landau equation as a model problem*, Lectures in Applied Mathematics, Vol. 31, pp. 141-190, AMS, Providence, 1996.
- [22] J. L. LIONS, E. MAGENES, *Non-Homogeneous Boundary Value Problems and Applications*, Volume 2, Springer, 1972.
- [23] J.L. LIONS, *Optimal Control of Systems Governed by Partial Differential Equations*, Springer, Berlin, 1971.
- [24] J.L. LIONS, *Control of Distributed Singular Systems*, Gauthier-Villars, Paris, 1985.
- [25] P. MANNEVILLE, *Dissipative Structures and Weak Turbulence*, Academic Press, 1990.
- [26] H. MAURER AND J. ZOWE, *First and second order necessary and sufficient optimality conditions for infinite-dimensional programming problems*, Mathematical Programming, 16, (1979) pp. 98–110, .
- [27] J.D. MURRAY, *Mathematical Biology*, Springer-Verlag, 1993.
- [28] P. NEITTAANMÄKI AND D. TIBA, *Optimal Control of Nonlinear Parabolic Systems*, Marcel Dekker, New York, 1994.
- [29] J. PAULLET, B. ERMENTROUT AND W. TROY, *The existence of spiral waves in an oscillatory reaction-diffusion system*, SIAM J. Appl. Math., 54(5) (1994), pp. 1386–1401.

- [30] J.P. RAYMOND, H. ZIDANI, *Hamiltonian Pontryagin's principles for control problems governed by semilinear parabolic equations*, Applied Mathematics and Optimization, 39 (1999), pp. 143–177.
- [31] J.A. SHERRATT, *On the evolution of periodic plane waves in reaction-diffusion systems of  $\lambda - \omega$  type*, SIAM J. Appl. Math., 54(5) (1994), pp. 1374–1385.
- [32] J. SMOLLER, *Shock Waves and Reaction-Diffusion Equations*, Springer-Verlag, 1994.
- [33] R. TEMAM, *Infinite-Dimensional Dynamical Systems in Mechanics and Physics*, Springer-Verlag, 1997.
- [34] F. TRÖLTZSCH, *Lipschitz stability of solutions of linear-quadratic parabolic control problems with respect to perturbations*, Dyn. Contin. Discrete and Impuls. Syst. Ser. A Math. Anal., 7(2) (2000), pp. 289–306
- [35] U. TROTTEBERG, C. OOSTERLEE, AND A. SCHÜLLER, *Multigrid*, Academic Press, London, 2001.